OPEN ACCESS
JOURNAL OF TELECOMMUNICATION, ELECTRONICS, AND CONTROL ENGINEERING (JTECE) ISSN: 2654-8275 (ONLINE)
JTECE. VOL. 08, NO. 02, PP.203-213, JULY 2026 DOI: 10.20895/JTECE.V8I2.2133

Numerical and Experimental Analysis of Electromagnetic Scattering Characteristics of Wood Beams and Wood Logs Using a UWB Vivaldi Antenna

Desi Ekowati[1], Mudrik Alaydrus*[,2]

[1,2]*Department of Electrical Engineering, Universitas Mercu Buana*
Jalan Meruya Selatan 1, Meruya Selatan, Jakarta, Indonesia

*[,2]Corresponding Author: mudrikalaydrus@mercubuana.ac.id
[1]fdekowati96@gmail.com

Received on 21-05-2026, accepted on 29-07-2026, published on 31-07-2026

Abstrak

Penelitian ini menyajikan investigasi numerik dan eksperimental terhadap karakteristik hamburan elektromagnetik balok kayu dan batang kayu mahoni (Swietenia macrophylla) menggunakan antena Vivaldi ultra-wideband (UWB). Antena Vivaldi UWB dengan rentang frekuensi operasi 0,89–10 GHz dirancang, difabrikasi, dan divalidasi melalui pengukuran koefisien refleksi serta pola radiasi. Selanjutnya, perilaku hamburan spesimen kayu dengan geometri dan orientasi yang berbeda dianalisis menggunakan simulasi elektromagnetik gelombang penuh serta pengukuran transmisi dengan konfigurasi dua antena. Hasil simulasi dan pengukuran menunjukkan kesesuaian yang baik, sehingga memvalidasi pendekatan yang diusulkan. Pada balok kayu, koefisien transmisi terukur berada di sekitar −40 dB pada 3 GHz, −45 dB pada 6 GHz, dan −60 dB pada 9 GHz, yang menunjukkan peningkatan atenuasi seiring bertambahnya frekuensi. Untuk batang kayu, spesimen berukuran kecil menghasilkan koefisien transmisi pada kisaran −35 hingga −45 dB, sedangkan batang berukuran besar menunjukkan atenuasi yang lebih tinggi, yaitu sekitar −45 hingga −65 dB, dengan pelemahan maksimum terjadi pada sudut rotasi 150°–250°. Hasil penelitian menunjukkan bahwa hamburan elektromagnetik sangat dipengaruhi oleh geometri, ukuran, orientasi, dan frekuensi operasi objek. Kombinasi pendekatan numerik dan eksperimental yang diterapkan menyediakan kerangka kerja yang andal untuk mengkarakterisasi interaksi gelombang elektromagnetik dengan struktur kayu. Temuan ini diharapkan dapat mendukung pengembangan lebih lanjut pada bidang penginderaan gelombang mikro, sistem radar, diagnostik kehutanan, serta pemodelan propagasi gelombang radio pada lingkungan bervegetasi.

Kata kunci: Hamburan elektromagnetik, balok kayu, batang kayu, antena UWB, antena Vivaldi, penginderaan gelombang mikro.

Abstract

This paper presents a numerical and experimental investigation of the electromagnetic scattering characteristics of mahogany (Swietenia macrophylla) wood beams and logs using an ultra-wideband (UWB) Vivaldi antenna. A UWB Vivaldi antenna operating over 0.89–10 GHz was designed, fabricated, and validated through reflection coefficient and radiation pattern measurements. The scattering behavior of wood specimens with different geometries and orientations was analyzed using full-wave electromagnetic simulations and controlled two-antenna transmission measurements. Good agreement between simulation and measurement confirms the validity of the proposed approach. For wood beams, the measured transmission coefficient was approximately −40 dB at 3 GHz, −45 dB at 6 GHz, and −60 dB at 9 GHz, indicating increased attenuation with frequency. For wood logs, the smaller specimen exhibited transmission levels of −35 to −45 dB, whereas the larger log produced −45 to −65 dB, with the strongest attenuation occurring between 150° and 250°. The results demonstrate that electromagnetic scattering is strongly influenced by object geometry, size, orientation, and operating frequency. The combined numerical and experimental methodology provides a reliable framework for characterizing electromagnetic interactions with wooden structures. These findings provide useful insight for microwave sensing, radar systems, forestry diagnostics, and vegetation-aware radio-wave propagation modeling.

Keywords: Electromagnetic scattering, wood beam, wood log, UWB antenna, Vivaldi antenna, microwave sensing.

I. INTRODUCTION

The interaction between electromagnetic waves and natural materials has attracted increasing attention in microwave sensing, radar systems, nondestructive testing, and wireless propagation studies. Wood is a particularly interesting natural dielectric material because its electromagnetic response depends strongly on its internal composition, moisture distribution, density, anisotropy, and structural heterogeneity [1], [2]. These properties influence attenuation, reflection, transmission, and scattering mechanisms, making wood characterization important for forestry monitoring, timber assessment, microwave sensing, and vegetation-aware communication modeling.

Among the various factors affecting the dielectric behavior of wood, moisture content is the most influential because water possesses a much higher dielectric constant than dry wood. Consequently, an increase in moisture content results in higher relative permittivity, greater dielectric loss, and stronger electromagnetic attenuation [1], [2], [18]. Wood density also contributes to the dielectric response, as denser wood generally exhibits a higher effective permittivity due to its larger solid volume fraction. Furthermore, wood is an inherently anisotropic material whose dielectric properties vary along the longitudinal, radial, and tangential grain directions. This anisotropy causes direction-dependent wave propagation and scattering characteristics, while natural variations in grain orientation, bark thickness, knots, and internal moisture distribution introduce additional structural heterogeneity. Therefore, accurate electromagnetic characterization of wood requires consideration of both its material properties and geometric features.

Wooden objects such as beams and logs are commonly encountered in engineered and natural environments. Wood beams are widely used in structural applications, whereas wood logs constitute naturally occurring cylindrical dielectric bodies frequently found in forested regions. Despite their practical importance, the electromagnetic scattering characteristics of these wooden structures over ultra-wideband (UWB) frequencies remain insufficiently understood. Variations in geometry, size, and rotational orientation can significantly modify wave propagation and scattering behavior, resulting in frequency-dependent transmission losses and angular scattering characteristics.

Ultra-wideband technology provides an effective framework for investigating complex dielectric materials because of its wide operating bandwidth, high temporal resolution, and good penetration capability [3], [4]. Broadband measurements enable the observation of frequency-dependent attenuation and scattering phenomena over multiple frequency bands, thereby providing more comprehensive information than narrowband techniques. Such measurements require antenna systems with wide impedance bandwidth, stable radiation characteristics, and sufficient directivity over the entire operating frequency range.

Among the available broadband antennas, the Vivaldi antenna has emerged as an attractive candidate for UWB sensing applications because of its wide impedance bandwidth, end-fire radiation pattern, planar configuration, high gain, and suitability for microwave imaging and radar systems [5]–[17]. Owing to these characteristics, Vivaldi antennas have been widely employed in ground-penetrating radar, biomedical imaging, through-wall sensing, moisture detection, and remote sensing applications. Their broadband performance also makes them well suited for investigating electromagnetic interactions with wooden structures across a wide frequency range.

Although considerable research has been conducted on the dielectric properties of wood, microwave imaging, tree inspection, and broadband Vivaldi antennas, most previous studies have focused either on material characterization, antenna development, or radar imaging independently. Comprehensive studies that combine full-wave electromagnetic simulations with controlled experimental measurements to investigate the scattering characteristics of wood beams and irregular wood logs over a broad UWB frequency range remain limited. In particular, the quantitative influence of object geometry, cross-sectional size, and rotational orientation on electromagnetic transmission attenuation has not been systematically investigated.

To address these limitations, this paper presents a combined numerical and experimental investigation of the electromagnetic scattering characteristics of mahogany (Swietenia macrophylla) wood beams and logs using an ultra-wideband (UWB) Vivaldi antenna. A broadband Vivaldi antenna operating over 0.89–10 GHz is designed, fabricated, and experimentally validated through reflection coefficient and radiation pattern measurements. Full-wave HFSS simulations and controlled two-antenna transmission measurements are subsequently performed to evaluate the influence of operating frequency, object geometry, cross-sectional size, and rotational orientation on electromagnetic propagation through wooden structures. The numerical model is validated through good agreement with experimental measurements, providing a practical framework for broadband characterization of electromagnetic wave interactions with wood.

The main contributions of this work are summarized as follows:

1. Design, fabrication, and experimental validation of a UWB Vivaldi antenna operating over 0.89–10 GHz for broadband electromagnetic scattering measurements.
2. Development of a combined numerical and experimental methodology for investigating the electromagnetic transmission and scattering characteristics of mahogany wood beams under different rotational orientations.
3. Quantitative comparison of two irregular mahogany wood logs with different cross-sectional dimensions to evaluate the influence of object geometry and size on electromagnetic attenuation over a broad frequency range.
4. Validation of the proposed HFSS model through good agreement between simulated and measured transmission characteristics, demonstrating the applicability of the proposed approach for broadband electromagnetic characterization of wooden structures.

II. LITERATURE REVIEW

The microwave characterization of wood has been extensively investigated because electromagnetic methods provide a non-contact and nondestructive means for material evaluation. Earlier studies reported that wood dielectric properties strongly depend on moisture content, frequency, and fiber orientation. Sahin and Ay [1] investigated dielectric properties of hardwood species at microwave frequencies, while Trubachev et al. [2] demonstrated anisotropic permittivity behavior in wood-based materials. These studies established the fundamental relationship between wood structure and microwave response.

Beyond dielectric characterization, microwave sensing methods have been explored for defect detection and tree health assessment. Ground-penetrating radar (GPR) and microwave tomography techniques have shown promising capability in identifying internal decay, cavities, and structural anomalies in tree trunks [7], [8]. Alhawari et al. [9] further demonstrated the use of microwave imaging combined with time-reversal processing for tree-trunk inspection. Although these methods provide valuable information regarding internal wood conditions, most studies focus on imaging or reconstruction performance rather than broadband scattering analysis.

Ultra-wideband systems have gained increasing importance in sensing and propagation studies because they enable broadband characterization of complex dielectric media. Their broad frequency coverage supports improved observation of frequency-dependent attenuation and scattering mechanisms [3], [4]. However, reliable UWB measurements require antenna systems capable of maintaining stable radiation and impedance characteristics across wide operating bandwidths.

Among broadband radiators, the Vivaldi antenna has been widely adopted in radar, imaging, and sensing applications. Amador et al. [5] reviewed the use of Vivaldi antennas in through-wall radar systems, emphasizing their directive radiation and broadband behavior. Similar advantages have been exploited in biomedical microwave imaging [10], [11], [12], ground-penetrating radar [13], [14], and environmental sensing applications [15], [16]. More recently, Cheng et al. [17] developed a dual-polarized high-gain Vivaldi antenna specifically for tree radar applications, demonstrating the suitability of this antenna type for vegetation-related electromagnetic measurements.

Despite the growing body of research on wood dielectric characterization, microwave imaging, and UWB antennas, relatively limited work has addressed the combined numerical and experimental investigation of electromagnetic scattering behavior of wood beams and wood logs using UWB Vivaldi antennas. In particular, the effects of object geometry, rotational orientation, and size variation on transmission and scattering responses remain insufficiently explored. This gap motivates the present study, which combines HFSS full-wave modeling and experimental measurements to analyze the electromagnetic behavior of wooden structures across multiple operating frequencies.

III. RESEARCH METHOD

A. Vivaldi Antenna

The profile of the Vivaldi antenna's slotline is described by an exponential curve of the form [7]:

$$y = A\, e^{bz} \tag{1}$$

A is set to 0.3 mm in order to obtain a slot line at the feed point of width 0.6 mm, whereas the exponential constant is determined through the lowest working frequency of the vivaldi antenna. Here we set f_L=0.89 GHz, and with the equation

$$f_L = \frac{c}{2\, W_{max}\sqrt{\varepsilon_{r,eff}}} \quad (2)$$

W_{max} is the opening of the taper at the end point, which is equal to two times of the value of y at the position z=115 mm. So that the value b=0.0441 is obtained.
The Vivaldi antenna was fabricated on an FR-4 epoxy substrate with a relative permittivity of $\varepsilon_r = 4.4$, dielectric loss tangent of $\tan\delta = 0.02$, and substrate thickness of 1.6 mm. A copper layer with a thickness of 35 µm was used as the conducting material. These substrate parameters were employed consistently in both the HFSS simulations and the fabricated prototype to ensure a direct comparison between numerical and experimental results.

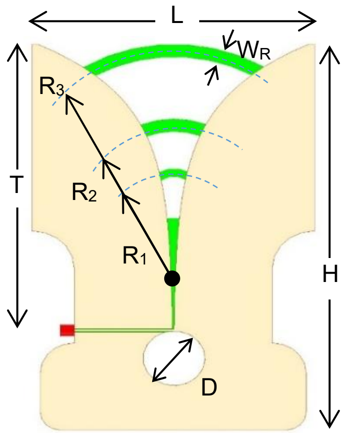

a)

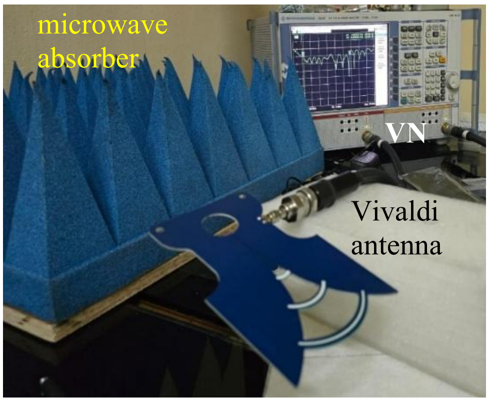

b)

Figure 1. a) Computer model of the designed Vivaldi antenna, b) Setup for measuring the reflection coefficient.

This exponential flare ensures smooth impedance transition from the feed to free space, so that the highest working frequency could be achieved with the feedline width and manufacturing precision of the feed line. The antenna is fed by a grounded coplanar waveguide with a width of w=0.75 mm and gap= 0.35 mm to match the characteristic impedance of 50 ohms with the given substrate. The final antenna geometry is illustrated in Fig. 1a). The overall antenna height is H = 155 mm, the flare length is T = 115 mm, and the antenna width is L = 100 mm. The exponential taper is defined by three reference radii R_1 = 8.5 mm, R_2 = 27.5 mm, and R_3 = 57.5 mm, while W_R = 3 mm denotes the flare edge width. A circular opening with diameter D = 11 mm is introduced between the coplanar-waveguide feed and the slotline to improve impedance matching. All dimensions are expressed in millimetres.
The characterization of the Vivaldi antenna was carried out using a vector network analyzer (VNA) in conjunction with microwave absorbers to minimize environmental interference, as depicted in Figure 1b). The antenna under test (AUT) was connected to the VNA through a precision coaxial cable, and a full two-port calibration was performed prior to measurement in order to eliminate systematic errors arising from cables and connectors. The VNA was configured to sweep across the frequency range of interest, ensuring coverage of the anticipated operational bandwidth of the antenna. To mitigate the effects of multipath propagation and spurious reflections, pyramidal microwave absorbers were placed in the vicinity of the AUT. These absorbers, composed of lossy dielectric foam, are designed to emulate free-space conditions by attenuating incident electromagnetic energy. Their placement around the antenna effectively reduced undesired reflections from nearby surfaces, thereby improving the accuracy of the measured scattering parameters.
During the measurement, the reflection coefficient (S11) was recorded to evaluate impedance matching and bandwidth characteristics of the Vivaldi antenna. Resonant frequencies were identified as those exhibiting distinct minima in the return loss response, corresponding to frequency bands where the antenna achieves efficient radiation. The acquired data were subsequently processed to validate the wideband performance of the antenna design and to confirm its suitability for ultra-wideband communication, radar, and electromagnetic sensing applications.

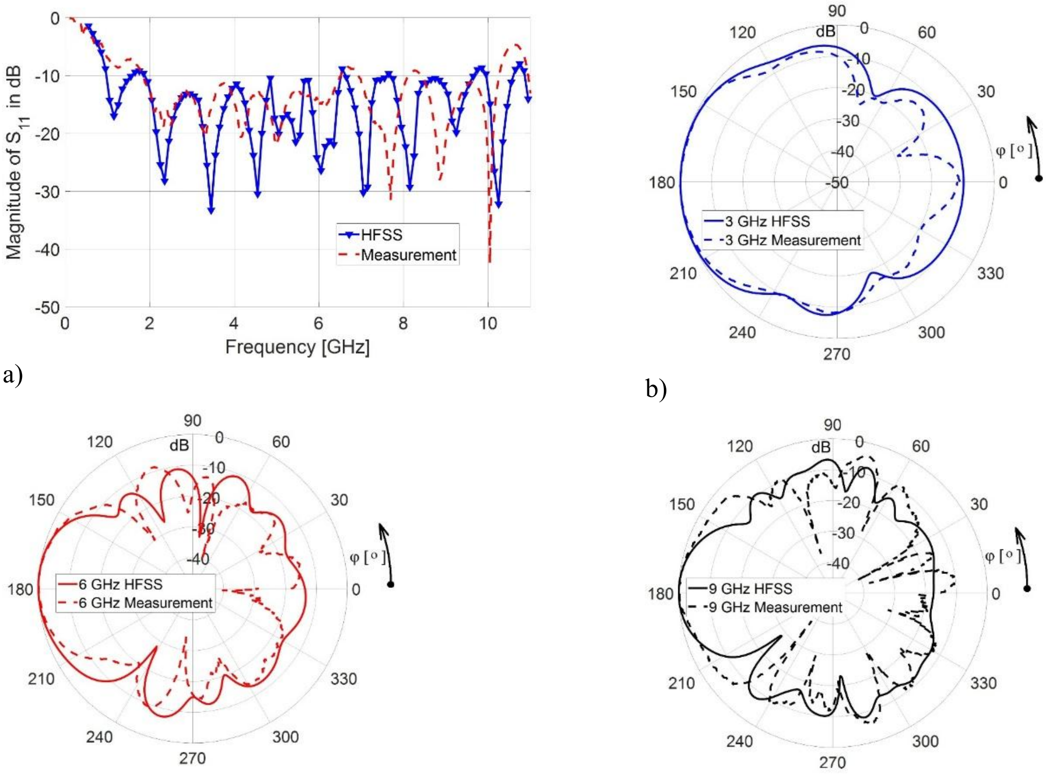

c) d)

Figure 2. a) Comparison calculated and measured reflection coefficient, b)-d) Comparison calculated and measured horizontal radiation pattern of Vivaldi antenna at 3, 6, 9 GHz.

Figure 2a) presents the comparison between the simulated and measured reflection coefficient S11 of the proposed structure. The blue curve with triangular markers represents the simulated results obtained from ANSYS HFSS, while the red dashed line corresponds to the experimental data measured using a vector network analyzer (VNA). The vertical axis indicates the magnitude of S11 in decibels (dB), where lower values represent better impedance matching, and the horizontal axis denotes the operating frequency in gigahertz (GHz). Both the simulation and measurement results clearly demonstrate the multiband nature of the design, as shown by the presence of several sharp resonances across the frequency range. At these resonance frequencies, the reflection coefficient dips below −10 dB, which is typically considered the threshold for good impedance matching. This implies that at multiple frequency bands, most of the input power is transmitted into the structure rather than reflected back, confirming effective operation. Overall, there is good agreement between the simulated and measured responses, as both show resonances occurring at nearly the same frequencies. However, some discrepancies are observed, particularly at higher frequencies above 7 GHz, where the measured results deviate slightly in resonance position and depth. These differences can be attributed to several practical factors such as fabrication tolerances, variations in material properties, connector losses, and environmental influences during measurement. In conclusion, the results validate the simulation and confirm that the proposed design achieves multiband operation with effective impedance matching. The minor differences between simulation and measurement are within acceptable limits, indicating that the fabricated prototype successfully realizes the intended electromagnetic performance.

Figures 2b)–d) compare the simulated and measured radiation patterns of the proposed Vivaldi antenna at 3, 6, and 9 GHz, respectively. In all cases, the measured results show good agreement with the HFSS simulations, confirming the validity of the antenna design and fabrication. At 3 GHz, the antenna exhibits a relatively broad radiation pattern with wide angular coverage and only minor deviations in the forward and backward directions. At 6 GHz, the radiation pattern becomes more complex with the appearance of multiple lobes, while the measured results continue to follow the overall simulated characteristics. At 9 GHz, additional side lobes are observed, resulting in a more irregular radiation profile; however, the measured and simulated patterns remain in good qualitative agreement. The small discrepancies observed across all frequencies, including differences in lobe amplitude and direction, are mainly attributed to fabrication tolerances, measurement alignment errors, connector and feeding losses, and residual reflections in the measurement environment. Overall, the close agreement between simulation and measurement demonstrates that the fabricated prototype successfully reproduces the predicted radiation characteristics over the entire 0.89–10 GHz operating band.

B. Observation of Wood block and Wood logging structures

Figure 3a) illustrates a simulated measurement setup designed to analyze the performance of the proposed antenna system in the presence of a dielectric obstacle. On both sides of the configuration, two identical antennas are positioned facing each other. These antennas serve as the transmitter and receiver, enabling the evaluation of transmission characteristics through the medium placed between them. The antennas are enclosed within a bounding box to define the simulation domain and to control the boundary conditions for accurate electromagnetic analysis. At the center of the setup lies a rectangular block, modeled in green, which represents a wooden object. The dimension of the wooden block is 40 mm x 40 mm x 540 mm. The wooden beam specimen was fabricated from air-dried mahogany (Swietenia macrophylla) with a moisture content of 12–18%. Based on reported dielectric properties of air-dried hardwoods at microwave frequencies, the relative permittivity of the wood was within the typical range: 2.8–3.4 [18] . Accordingly, all HFSS simulations of the wood beams and wood logs employed material parameters of $\varepsilon_r = 3$ and $\sigma = 0.0047$ S/m. This setup can be used to assess important parameters such as attenuation, scattering, and possible frequency-dependent losses introduced by the wood. The overall arrangement mimics a free-space measurement scenario, where the antennas radiate and receive electromagnetic waves with the block acting as the object under investigation. By comparing the transmission data with and without the block, the dielectric properties of the wood can be characterized. Such a setup is valuable in applications such as through-material sensing, nondestructive testing, and communication studies involving natural obstructions.

Figure 3b) illustrates a schematic of the experimental setup used to investigate the effect of a wooden block on electromagnetic wave propagation. Two antennas, labeled as Antenna 1 and Antenna 2, are placed facing each other at a fixed distance of 80 cm. These antennas function as the transmitter and receiver, respectively, with the electromagnetic signal propagating along the dashed blue line between them. At the midpoint of this path, a wooden block is positioned as the material under test.

The lower part of the figure shows two orientations of the wooden block. On the left, the block is aligned with its edges parallel to the coordinate axes, corresponding to a rotation angle of α=0∘. On the right, the block is rotated by 45 degrees, such that its diagonal aligns with the propagation path, corresponding to α=45∘. This variation in orientation is important because it changes the effective thickness and geometry of the material encountered by the propagating electromagnetic wave.

By measuring the transmission between the two antennas for these different orientations, the experiment allows the evaluation of how the block's rotation influences the attenuation and scattering of the wave. This provides useful insight into the anisotropic behavior of dielectric materials like wood when interacting with electromagnetic signals. Such a setup is relevant for studies in wave propagation through natural materials, nondestructive testing, and wireless communication scenarios where obstacles are present.

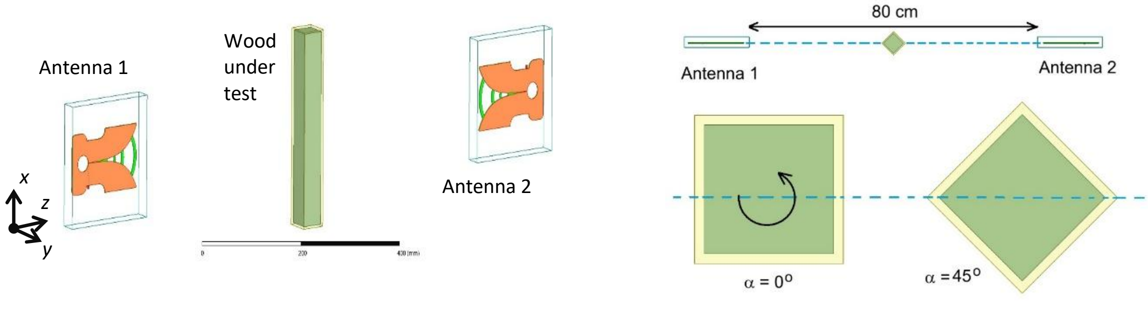

a) b)

Figure 3. HFSS model for observing scattering characteristic of a wood block, a) basic configuration, b) rotating the wood block around its axis.

IV. RESULTS AND DISCUSSION

This picture in Figure 4a) shows the experimental setup for measuring the effect of wood on electromagnetic wave propagation. Two identical antennas, labeled as antenna 1 (transmitting antenna) and antenna 2 (receiving antenna), are positioned facing each other. This configuration enables the evaluation of the signal behaviour under the investigated conditions. At the center of the setup, a vertical wooden beam is mounted as the material under test. The wood is fixed on top of a rotating table, which allows precise adjustment of its orientation. By rotating the beam to different angles, the effect of the thickness and geometry of the obstacle to the transmission of electromagnetic waves can be studied. The environment is surrounded by blue RF absorbers, which are designed to minimize reflections and external interference. This ensures that the measured signals correspond primarily to the direct interaction between the antennas and the wooden block, rather than being distorted by unwanted reflections from the laboratory walls or equipment.

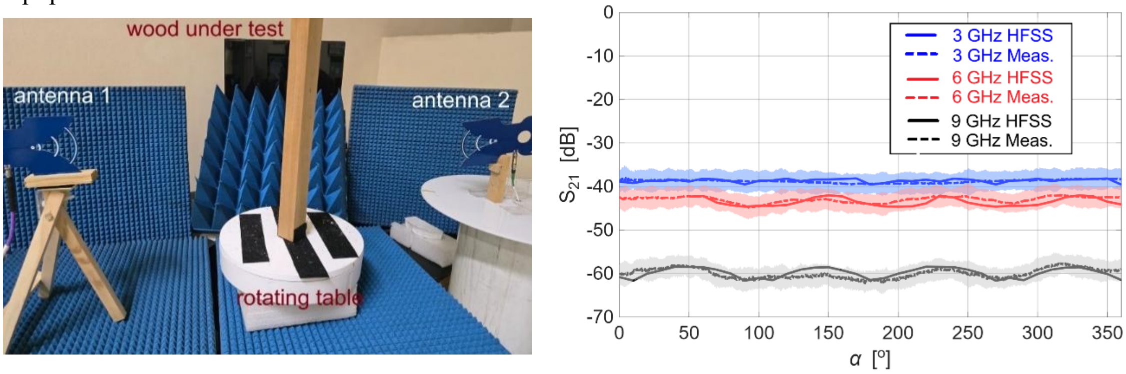

a) b)

Figure 4. a) Measurement setup for observation the effect of wood beam to transmission coefficient, b) comparison of calculated and measured transmission coefficient as function of angle at different signal frequency.

Figure 4b) shows the simulated and measured transmission coefficients (S_{21}) as a function of the rotation angle of the wooden beam at three different frequencies: 3 GHz, 6 GHz, and 9 GHz. The solid curves represent the results obtained from HFSS simulations, while the dashed curves correspond to the experimental measurements. The vertical axis indicates the transmission magnitude in decibels (dB), and the horizontal axis represents the rotation angle of the block from 0° to 360°.

At 3 GHz, both the simulated and measured values of S21 remain relatively stable around −40 dB across all rotation angles. This suggests that the orientation of the wood beam has little influence on wave transmission at lower frequencies, where the wavelength is much larger than the cross-sectional dimension of the wood. The close overlap between simulation and measurement further confirms the accuracy of the numerical model in capturing the material's behavior.

At 6 GHz, the transmission levels drop slightly to around −45 dB. Small variations appear as the wood beam is rotated, reflecting a moderate influence of geometry on the propagation at this frequency. The measured results follow the simulated trend closely, though minor discrepancies are observed in certain angular regions. These deviations can be attributed to measurement uncertainties, alignment imperfections, or inhomogeneities in the wooden beam.

At 9 GHz, the transmission loss is much more pronounced, with S21 values averaging around −60 dB. This indicates that at higher frequencies, the wood introduces stronger attenuation, as the wavelength is now comparable to the beam's dimensions and dielectric effects become more significant. The measured and simulated curves show good agreement, though the measured data exhibit slightly higher fluctuations, which may result from environmental reflections or increased sensitivity of the setup at higher frequencies.

In summary, the results confirm that the wooden block has a frequency-dependent effect on electromagnetic transmission. At low frequencies, its influence is minimal, while at higher frequencies, significant attenuation occurs. The close agreement between HFSS simulations and measurements validates the reliability of the proposed model and confirms the experimental observations.

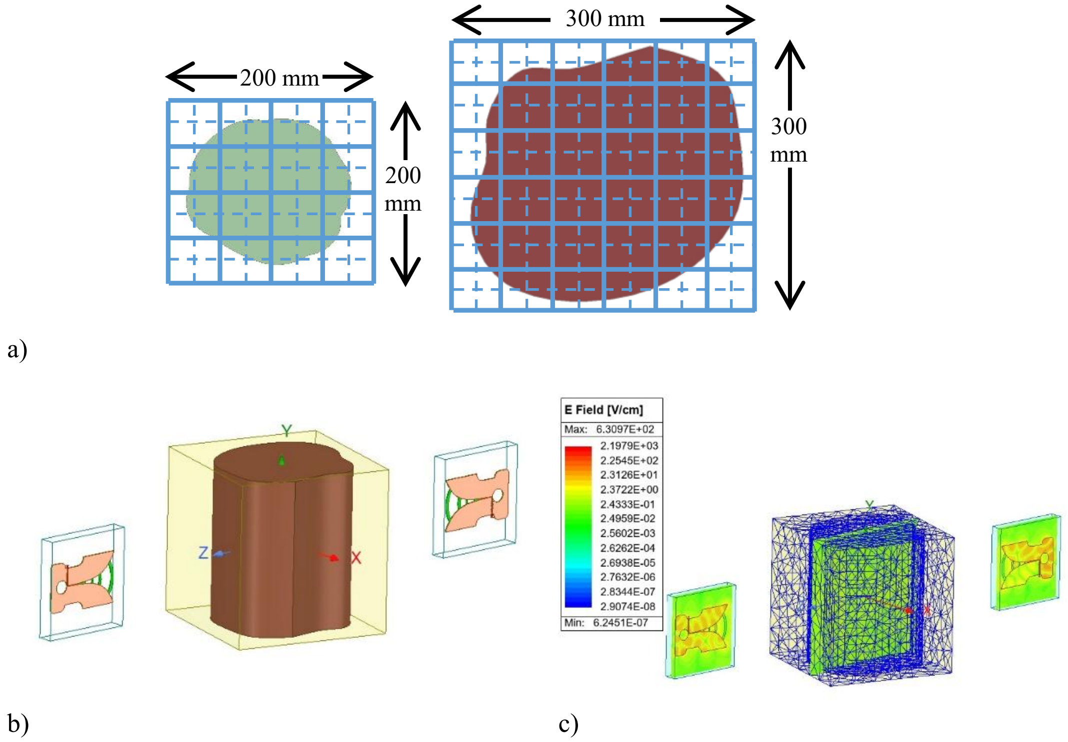

Figure 5. HFSS model of the wood-log scattering experiment: a) detailed dimension of the logs with height 500 mm, b) simulation geometry consisting of two opposing UWB Vivaldi antennas and a cylindrical wood log, c) adaptive mesh and electric-field distribution showing electromagnetic interaction with the wooden object.

Figure 5a) presents the cross-sectional geometries of the two mahogany (Swietenia macrophylla) wood log specimens used in the electromagnetic simulations. Both logs have a length (height) of 500 mm, while their cross-sections were normalized to 200 mm × 200 mm and 300 mm × 300 mm analysis domains for the smaller and larger specimens, respectively. A square raster grid with uniform spacing was superimposed on each cross-section to facilitate dimensional measurements, geometric characterization, and numerical discretization. The dashed lines indicate the centers of the grid cells, providing reference points for coordinate extraction. This raster representation enables consistent comparison between specimens of different sizes and serves as the basis for constructing the computational models used in the electromagnetic scattering simulations. Figure 5b) presents the numerical configuration employed for evaluating electromagnetic wave interaction with a wood log using UWB Vivaldi antennas. The simulation model consists of two identical antennas positioned symmetrically around a cylindrical wooden sample inside an air-filled computational domain. The electric-field distribution, in Figure 5c), indicates that the radiated energy propagates through the wood while undergoing attenuation and scattering due to the dielectric properties and geometry of the log. The accompanying mesh plot demonstrates the adaptive discretization used in HFSS to ensure accurate full-wave analysis of the antenna–wood interaction.

The measurement setup in Figure 6a) is designed to investigate how electromagnetic waves interact with a natural object, in this case a tree log, under controlled conditions. The environment is surrounded by blue RF absorbers on the floor and walls, which reduce unwanted reflections and create conditions close to free space. At both sides of the setup, two identical wideband Vivaldi antennas are placed facing the log, one functioning as the transmitter and the other as the receiver. The log itself is mounted vertically on a rotating platform, which allows angular measurements by turning the object to different orientations relative to the antennas. During operation, the transmitting antenna radiates a signal toward the log, and the receiving antenna collects the transmitted or scattered signal after interaction with the wood. By rotating the log and recording the received signals at different angles, the setup enables characterization of attenuation, scattering, and transmission properties of the tree log. Such measurements are often used in wireless communication studies, radar cross-section analysis, and channel modeling in environments where vegetation significantly affects signal propagation. Here, two different wood logs are observed.

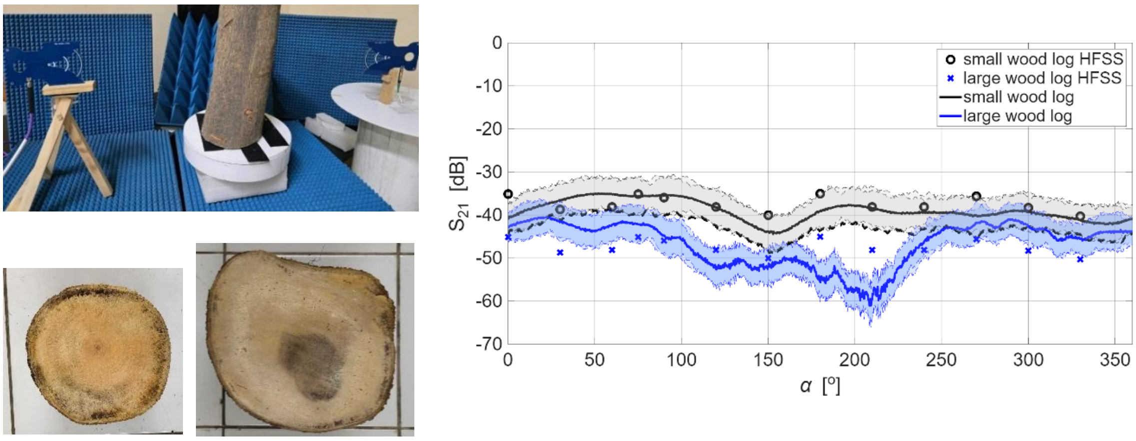

a) b)

Figure 6. a) Measurement setup for wood log and two different wood logs, b) comparison of transmission coefficient for small and large wood logs.

The measurement results presented in Figure 6b) illustrate the transmission coefficient S_{21} as a function of rotation angle for two wood logs of different sizes. At each rotation angle, ten independent measurements were performed using the vector network analyzer. The mean value and standard deviation of the measured S_{21}were subsequently calculated. In Figure 6b), the solid curves represent the mean measured values, while the shaded regions indicate the corresponding standard deviation, illustrating the measurement variability. The obtained curves reveal that both objects introduce significant attenuation compared to free-space transmission, thereby confirming the strong interaction between electromagnetic waves and vegetative obstructions.

For the small wood log (black curve), the measured transmission coefficient varies between approximately −35 dB and −45 dB over the entire rotation range. The relatively narrow standard deviation indicates good measurement repeatability and suggests that the smaller log produces only modest changes in the propagation path as its orientation varies. Although the log attenuates the propagating signal, a considerable portion of the incident energy is still transmitted or diffracted around the object. In contrast, the large wood log (blue curve) exhibits substantially stronger attenuation, with measured S_{21} values ranging from approximately −45 dB to −65 dB. The most pronounced attenuation occurs between 150° and 250°, where the received signal reaches its minimum. Compared with the smaller specimen, the larger log also exhibits a wider standard deviation in this angular region, indicating greater measurement variability associated with its irregular geometry and stronger electromagnetic interaction. The more noticeable variation of S_{21} with rotation further highlights the influence of the log's larger cross-sectional area, irregular shape, bark thickness, and moisture distribution on wave propagation.

Overall, the comparison between the two measurements confirms that log size and orientation are critical factors influencing wave propagation through vegetation. Larger logs introduce stronger attenuation, while rotational dependence indicates that vegetation cannot be modeled as an isotropic medium. These findings are particularly relevant for the accurate modeling of radio-wave propagation in forested or vegetated environments, where vegetation-induced shadowing, scattering, and absorption significantly affect the performance of communication and radar systems.

V. CONCLUSION

This study presented a combined numerical and experimental investigation of the electromagnetic scattering characteristics of mahogany (Swietenia macrophylla) wood beams and wood logs using a UWB Vivaldi antenna. The proposed antenna was successfully designed, fabricated, and experimentally validated, achieving an operating frequency range of 0.89–10 GHz with good agreement between the simulated and measured reflection coefficients and radiation patterns. The electromagnetic interaction between wooden structures and incident waves was investigated through HFSS simulations and transmission measurements using a two-antenna configuration.

For the wood beam, the measured transmission coefficient was approximately −40 dB at 3 GHz, −45 dB at 6 GHz, and −60 dB at 9 GHz, demonstrating progressively stronger attenuation with increasing frequency. For the wood logs, the smaller specimen exhibited transmission levels ranging from approximately −35 to −45 dB, whereas the larger specimen produced significantly higher attenuation of approximately −45 to −65 dB, with the maximum attenuation occurring between 150° and 250°. The experimental results showed good qualitative agreement with the numerical simulations over the entire measurement range, confirming the validity of the proposed electromagnetic model and measurement methodology.

The results demonstrate that electromagnetic scattering from wood is strongly influenced by operating frequency, object size, geometry, and rotational orientation. Compared with the smaller log, the larger specimen consistently produced approximately 10–20 dB greater transmission loss, indicating the significant influence of cross-sectional dimensions on electromagnetic propagation. It should be noted that these attenuation values were obtained from air-dried mahogany specimens with a moisture content of approximately 12–18%. Consequently, the reported results are specific to the tested material condition and should not be considered universally representative of all wood species or moisture conditions. Since moisture content was not systematically varied or controlled during this study, its influence on the electromagnetic scattering characteristics could not be quantitatively evaluated.

These findings provide valuable insight into wave interaction with wooden materials and support future developments in nondestructive material characterization, microwave sensing, forestry monitoring, vegetation-aware wireless communication, and radar-based environmental applications. Future work will investigate the effects of controlled moisture content, dielectric property extraction, radar cross-section analysis, and tomographic reconstruction techniques to achieve a more comprehensive electromagnetic characterization of wooden media under varying environmental conditions.

ACKNOWLEDGMENT

This research was supported by the Directorate of Research and Community Service (DPPM), Ministry of Higher Education, Science, and Technology (Kemdiktisaintek), Republic of Indonesia, under the Penelitian Tesis Magister research grant program No. 0988/LL3/AL.04/2025; 01-1-4/030/SPK-RISET/VI/2025 for the fiscal year 2025.

AUTHOR CONTRIBUTION

MA constructed the study design. DE performed and analyzed the data. DE prepared the manuscript and revised the final version of the paper. MA and DE have read the final manuscript and approved the submission.

REFERENCES

[1] H. Şahin and N. Ay, "Dielectric properties of hardwood species at microwave frequencies," J. Wood Sci., vol. 49, no. 3, pp. 242–247, 2003.
[2] A. Trubachev et al., "Microwave complex permittivity and anisotropy of conifer wood chips," J. Wood Sci., vol. 68, no. 1, Art. no. 32, 2022.
[3] T. Saeidi, I. Ismail, R. H. Adam, A. R. H. Alhawari, and W. P. Wen, "Ultra-wideband elliptical patch antenna for microwave imaging of wood," Int. J. Microw. Wireless Technol., vol. 11, no. 9, pp. 917–925, 2019.
[4] M. Sudakova et al., "Assessment of health status of tree trunks using ground penetrating radar tomography," AIMS Geosci., vol. 7, no. 2, pp. 162–179, 2021.
[5] F. Tosti et al., "The use of GPR and microwave tomography for the assessment of the internal structure of hollow trees," IEEE Trans. Geosci. Remote Sens., vol. 60, Art. no. 2002314, 2022.
[6] A. R. H. Alhawari et al., "Health control of tree trunk utilizing microwave imaging and time reversal," ACS Omega, vol. 8, no. 18, pp. 14387–14400, 2023.
[7] G. Amador et al., "Overview of Vivaldi antenna selection for through-wall radar," Sensors, vol. 24, no. 18, Art. no. 6073, 2024.
[8] J. Ghimire et al., "Vivaldi antenna arrays fed by frequency-independent networks," Sensors, vol. 21, no. 14, Art. no. 4779, 2021.
[9] M. Slimi et al., "Metamaterial Vivaldi antenna array for breast cancer detection," Sensors, vol. 22, no. 9, Art. no. 3319, 2022.
[10] Ş. Yıldız and M. B. Kurt, "Breast cancer detection using a high-performance ultra-wideband Vivaldi antenna," Appl. Sci., vol. 15, no. 11, Art. no. 6044, 2025.
[11] A. M. Qashlan et al., "A modified compact flexible Vivaldi antenna array design for microwave imaging applications," Appl. Sci., vol. 12, no. 10, Art. no. 5040, 2022.
[12] M. V. L. Bhavani, D. Chaturvedi, T. Lanka, T. A. Raju, G. Rana, and A. Kumar, "A noninvasive microwave imaging system for breast tumor detection using a high-gain Vivaldi antenna array sensor," IEEE Sensors J., vol. 25, no. 17, pp. 32631–32640, Sept. 2025.
[13] K. P. K. Riyanti, E. Setijadi, N. Nurhayati, and G. Hendrantoro, "Single-feed dual-aperture Vivaldi antenna for GPR detection of arbitrarily oriented objects," IEEE Antennas Wireless Propag. Lett., early access, 2026.
[14] H. S. Senapati, P. Chongder, and S. Maiti, "Design and simulation of a parasitic patch loaded novel broadband antipodal Vivaldi antenna for GPR applications," in Proc. IEEE Microw., Antennas Propag. Conf. (MAPCON), Bangalore, India, 2022, pp. 886–890.

[15] M. Nasir et al., "Broadband dual-podal multilayer Vivaldi antenna array for remote sensing applications," IET Microw., Antennas Propag., vol. 17, no. 7, pp. 505–517, 2023.
[16] F. Stern, W. Taute, R. Knöchel, and M. Höft, "Dual antipodal Vivaldi antenna-based moisture sensor for industrial process control," IEEE Sensors J., vol. 23, no. 19, pp. 22430–22439, Oct. 2023.
[17] K. Cheng et al., "A compact dual-polarized Vivaldi antenna with high gain for tree radar applications," Sensors, vol. 24, no. 13, Art. no. 4170, 2024.
[18] R. Olmi, M. Bini, A. Ignesti, and C. Riminesi, "Dielectric properties of wood from 2 to 3 GHz," J. Microw. Power Electromagn. Energy, vol. 35, no. 3, pp. 135–143, 2000.